P2.7 USING OBSERVATIONS TO DEVELOP, INITIALIZE, AND VALIDATE TWO LAND-SURFACE SCHEMES WITHIN ARPS

J. A. Brotzge* and D. Weber

Center for Analysis and Prediction of Storms
University of Oklahoma

1. INTRODUCTION

Land-surface model schemes (LSMs) are designed to simulate the exchange of surface water and energy fluxes at the soil-atmosphere interface. Of the many such LSMs in use today, most differ in computational philosophies and in model physics and parameterizations (Henderson-Sellers et al. 1993). One method to determine which schemes best model land-surface exchange processes is by comparison of model output to long-term, point-scale observational data (e.g., Betts et al. 1993, Betts et al. 1997, Chen et al. 1997; Qu et al. 1998). Ideally, these observations are used to validate, and then improve, the model physics.

A comprehensive set of surface observations have been collected in real-time at ten sites across Oklahoma since January 2000. These data include 5-minute observations of standard atmospheric data, soil temperature and moisture, skin temperature, and radiation and flux data. These data were used to initialize, force, and evaluate the two land-surface schemes available within the Advanced Regional Prediction System (ARPS) model (Xue et al. 2000 and Xue et al. 2001) developed by the Center for Analysis and Prediction of Storms (CAPS) at the University of Oklahoma.

The ARPS was originally designed with the Interactions Soil Biosphere Atmosphere (ISBA) scheme (Noilhan and Planton 1989), a "force-restore" land-surface model (LSM). A second LSM option now available in ARPS, dubbed "OUSoil", is a slightly modified version of the OSU-NOAH LSM (Ek and Mahrt 1991) used operationally by the ETA model. The purpose of this study is to evaluate the performance of each scheme, and highlight the value of using observations to develop and improve model performance. The first set of numerical experiments involve running one-dimensional forecasts twenty-four hours using OASIS, Mesonet, and NWS sounding data for initialization and atmospheric variables for forcing. The LSM was allowed to evolve and the model predicted soil temperature and moisture and surface-layer fluxes were later compared to observations. The second set of experiments incorporated the fully coupled 3-D ARPS configuration. The model domain included the Southern Great Plains with a horizontal resolution of 32 km. Model predicted near surface temperature variables were compared against ASOS observations.

* Corresponding author address: Jerald A. Brotzge, CAPS/University of Oklahoma
100 E. Boyd, Suite #1110 Norman, OK 73019;
E-mail: jbrotzge@ou.edu.

2. ARPS LSM DESCRIPTIONS

2.1 The Interaction Soil Biosphere Atmosphere (ISBA) scheme

Several improvements have been incorporated into the original ISBA scheme based on results from Pleim and Xiu (1995) and Xiu and Pleim (2001). Brotzge and Weber (2002) describe preliminary results of validation of the ISBA scheme using Mesonet and OASIS observations. The model soil dynamics of the ISBA scheme are briefly described in Section 2.1.1, and the land surface physics are described in Section 2.1.2.

2.1.1 Model soil dynamics

The Interaction Soil Biosphere Atmosphere scheme is a "force-restore" method following Deardorff (1978) and is limited to five prognostic equations for soil temperature and moisture (Noilhan and Planton 1989; Pleim and Xiu 1995). These five equations provide memory from the land surface to the atmospheric system. These five prognostic equations are:

$$\frac{\partial T_s}{\partial t} = \lambda_T \left(Rn - LE - H\right) - \frac{2\pi}{\tau}\left(T_s - T_2\right) \quad (1)$$

$$\frac{\partial T_2}{\partial t} = \frac{1}{\tau}\left(T_s - T_2\right) \quad (2)$$

$$\frac{\partial w_g}{\partial t} = \frac{C_1}{\rho_w d_1}\left(P_g - E_g\right) - \frac{C_2}{\tau}\left(w_g - w_{geq}\right) \quad (3)$$

$$\frac{\partial w_2}{\partial t} = \frac{1}{\rho_w d_2}\left(P_g - E_g - E_{tr}\right) \quad (4)$$

$$\frac{\partial w_r}{\partial t} = \sigma_f P - \left(E_c - E_{tr}\right) - R_r \quad (5)$$

where the five prognostic variables include the surface skin temperature (T_s), the mean-layer soil temperature (T_2), the ground surface wetness (w_g), the mean-layer root zone soil moisture (w_2), and canopy wetness (w_r). These time-dependent parameters are forced by the net radiation (R_n), precipitation (P), bare soil evaporation (E_g), canopy evaporation (E_c), and evapotranspiration (E_{tr}) in the form of latent heat flux (LE), sensible heat flux (H), and surface runoff (R). The variable w_{geq} is the surface volumetric water content, which balances capillary forces and is estimated by Noilhan and Planton (1989) as a function of soil type. The surface temperature and moisture are restored to equilibrium by heat and moisture sources from the soil layers below. The time scale at which these variables act is prescribed a priori in the form of a time constant τ (set to one day for our tests). Note that this scheme allows for only two soil levels, and the depths of these soil layers also are predetermined (d_1 = 0.1 m; d_2 = 0.9 m). The interaction between the soil and atmosphere varies as a function of the fractional vegetation cover (σ_f), vegetation type, soil type, heat capacity (C_1 and C_2), and thermal conductivity (λ_T).

2.1.2 Land surface physics

Noilhan and Planton (1989) defined the land surface physics used within the ISBA scheme. The net radiation is estimated from

$$Rn = SW_{in}(1-\alpha) + \varepsilon\left(LW_{in} - \sigma T_s^4\right) \tag{6}$$

where SW_{in} and LW_{in} is the incoming shortwave and longwave radiation, respectively. The sensible heat flux is estimated as

$$H = \rho C_p C_H V(T_s - T_a) \tag{7}$$

with ρ the air density, C_p the specific heat at constant pressure, C_H is the drag coefficient, V is wind speed at 2 m, and T_a is the air temperature. The latent heat flux is defined as the sum of the bare ground and canopy evaporation and transpiration:

$$LE = L_v(E_g + E_c + E_{tr}) \tag{8}$$

and L_v is the latent heat of vaporization. The bare ground and canopy evaporation are defined as

$$E_g = (1-veg)\rho C_p V\left[h_u q_{sat}(T_s) - q\right] \tag{9}$$

$$E_c = \sigma_f \rho F_w \left[q_{sat}(T_s) - q\right] R_a^{-1} \tag{10}$$

where h_u is the relative humidity at the ground surface, q is the specific humidity, q_s is the saturated specific humidity, F_w is the fraction of the canopy that is wet, and R_a is the aerodynamic resistance (s m^{-1}). The evapotranspiration is defined similarly as

$$E_{tr} = veg\rho(1-F_w)\left[q_{sat}(T_s) - q\right](R_a + R_s)^{-1} \tag{11}$$

with R_s the surface resistance (s m^{-1}) as defined explicitly by Noilhan and Planton (1989). Ground heat flux is estimated analytically using

$$G = \frac{2\pi}{\tau C_p}(T_s - T_2) + \frac{1}{\lambda_T}\frac{\partial T_s}{\partial t}. \tag{12}$$

2.2 The OUSoil scheme

The OUSoil scheme was developed largely based on the Noah Land Model, Version 2.3.2 (Ek and Mahrt 1991; K. Mitchell and M. Ek 2002, personal communication) and implemented into ARPS during the summer of 2002. Components describing the snow and ice physics processes are not part of the updated model at the time of manuscript preparation, but will be incorporated into the model at a later date. A number of modifications were made to the scheme to allow for multiple soil levels and grid stretching within the soil column.

2.2.1 Model soil dynamics

The model soil dynamics for temperature are governed by the diffusion equation

$$(\rho C)_i \frac{\partial T}{\partial t} = \frac{\partial}{\partial z}\left(\lambda_T \frac{\partial T}{\partial z}\right) \tag{13}$$

as a function of the soil heat capacity and thermal conductivity. The total heat capacity (C) of the soil is computed as a function of the soil water content, η (m^3 m^{-3}), and the volumetric heat capacities of soil (C_{soil}), water (C_{water}), and air (C_{air}) and is given by:

$$C = \eta C_{water} + (1-\eta_{sat})C_{soil} + (\eta_{sat} - \eta)C_{air} \tag{14}$$

The heat capacity varies as a function of soil type. The maximum holding capacity of water for a particular soil type is expressed implicitly through use of the saturated soil water content, η_{sat} (m^3 m^{-3}).

Two options are available within OUSoil for computing soil thermal conductivity. The first option, described by McCumber and Pielke (1981), is a relatively simple logarithmic relationship between thermal conductivity and soil water potential. A second method for estimating soil thermal conductivity is described by Peters-Lidard et al. (1998).

The model soil dynamics for moisture is estimated from the diffusion equation,

$$\frac{\partial \eta}{\partial t} = \frac{\partial}{\partial z}\left(D_\eta \frac{\partial \eta}{\partial z} \right) + \frac{\partial K}{\partial t} \quad (15)$$

as defined by Chen and Dudhia (2001) where D is soil water diffusivity, and K is the hydraulic conductivity. Smirnova et al. (1997) defines the soil water diffusivity as

$$D_\eta = \frac{-bK_{\eta_s}\psi_s}{\eta}\left(\frac{\eta}{\eta_s}\right)^{b+3} \quad (16)$$

where η_s is the saturated soil water content, ψ_s is the saturated soil potential, and $K_{\eta s}$ is the saturated hydraulic conductivity. A linearization of the saturated hydraulic conductivity equation was estimated by Smirnova et al. (1997) as

$$K'_{\eta s} = \left(\frac{K_{\eta s}}{\eta_s}\right)\left(\frac{\eta^\eta}{\eta_s}\right)^{2b+2} \quad (17)$$

2.2.2 Land surface physics

The land surface physics of OUSoil are described by Ek and Mahrt (1991). The skin temperature is the primary interface between the soil and atmosphere and is the driving force of the entire surface energy budget. Ek and Mahrt (1991) derive the skin temperature, T_s, from the sensible heat flux equation, and the potential evaporation, E_p, as:

$$T_s = \frac{T_a + \left(1/1+r\right)\left(\theta_a - T_a\right) + \left(1/1+r\right)\left(\frac{1}{rC_hC_p}\right)\left(F - \sigma T_a^4 - LE + \frac{K_t T_{soil}}{\Delta z}\right)}{\left(1/1+r\right)\left(\frac{1}{\rho C_h C_p}\right)\left(\frac{K_t}{\Delta z}\right) + 1} \quad (18)$$

$$E_p = \frac{\rho C_p C_h}{L_v}\left(\frac{\left(R_n \Delta / \rho C_p C_h\right) + \left(\theta_a - T_a\right)\Delta + (r+1)\left(q_a^* - q_a\right)\frac{L_v}{C_p}}{\Delta + (r+1)} \right) \quad (19)$$

where F is the radiative forcing, Δz is the thickness of the top soil layer, and r is a variable defined as a function of surface pressure and temperature as

$$r = \frac{4\sigma T_a^4 R_d}{p_{sfc} C_p C_h} \quad (20)$$

The radiative forcing is defined as

$$F = (1-\alpha)SW_{in} + LW_{in}$$

where α is the surface albedo. The latent heat flux is computed as a fraction of the potential evaporation, E_p. The R_n is defined as in Eq. (6), q_a* is the saturation specific humidity of the air, q_a is the actual air specific humidity, and Δ is defined as

$$\Delta = \frac{dq_s^*}{dT}\frac{L_v}{C_p} \quad (21)$$

where q_s* is the skin saturation specific humidity. The latent heat flux is estimated as in Eq. (8). However, the bare ground, canopy, and transpiration terms are calculated as

$$E_g = (1-\sigma_f)\beta E_p \quad (22)$$

$$E_c = \sigma_f E_p \left(\frac{W_c}{S}\right)^{0.5} \quad (23)$$

$$E_{tr} = \sigma_f E_p R_c \left[1 - \left(\frac{W_c}{S}\right)^{0.5}\right] \quad (24)$$

The β term in Eq. (23) is a weighting factor estimated as a function of soil water availability and defined as

$$\beta = \frac{\eta - \eta_w}{\eta_{fc} - \eta_w} \tag{25}$$

where η_w is the wilting point and η_{fc} is the field capacity. The canopy resistance, R_c, is defined by Ek and Mahrt (1991).. The sensible heat flux is estimated as given in Eq. (7), and the ground heat flux is computed at the top-soil layer by

$$G = K_T \frac{(\theta_s - T_{soil})}{\Delta z} \tag{26}$$

where T_{soil} is the soil temperature at the bottom of the soil layer and Δz is the soil layer thickness..

3. EXPERIMENT DESCRIPTION

To adequately evaluate the performance of the ARPS LSM schemes, a series of 1-D uncoupled tests were conducted, followed by real-time fully-coupled 3-D testing. To accommodate the new code and solution structure, a new complement of input parameters was implemented into the ARPS code to permit additional functionality and stand-alone testing of the LSMs.

3.1 One-dimensional experiments

For the 1-D tests, several clear days were chosen from the one-year data set. Data from 20 May, 2000, represented a synoptically quiescent spring day characterized by warm temperatures (maximum temperature near 28 °C), a moderately moist soil and vigorous vegetation growth (NDVI=0.61). High pressure also dominated during 1-2 August, 2000, and represented a soil moisture depletion period with similar soil wetness but elevated air temperatures (maximum air temperature of 37 °C) and stressed vegetation (NDVI = 0.5). Forecasts were initialized from observations of soil temperature and moisture at 4 depths within the soil column. The atmospheric variables were initialized using the 00 UTC Norman, Oklahoma sounding. During the 12-hour simulation the model run was forced at 5-minute intervals with observed solar radiation, air temperature, and relative humidity. The ISBA simulations utilized two soil levels, 10 and 90 cm in thickness. The soil model resolution for the newly implemented LSM varied between 10 and 90 levels, depending on the forecast site and season. This configuration allowed only the soil model and atmospheric flux variables to vary, and therefore verification efforts focused primarily on the performance of the LSMs. Results of these tests are described in Section 4.2.

3.2 Three-dimensional real-time experiments

Real-time operational testing of the soil schemes began during the summer of 2002. The new soil model was tested at a grid resolution of 32 km over the Central US region (2000 km x 2000 km) with a forecast length of 24 hours. Initialization of the atmospheric state was performed by the ARPS Data Analysis System (ADAS) and included synoptic surface and upper air observations as well as Oklahoma Mesonet, wind profiler, Doppler radar derived winds, and aircraft observations. The soil temperature and moisture fields were initialized from the ETA model forecast. The ISBA configuration used the standard 2 soil levels, the top layer 10 cm thick and the root zone layer 90 cm deep. The OUSoil LSM simulations were conducted with 20 soil levels, each 5 cm thick, following the one-dimensional test configuration. Results from the fully-coupled, 3-D model simulations are presented in Section 4.3.

4. LSM VALIDATION

A key element of any research study is the verification of a model or method and within this report, we utilize the OASIS and Mesonet data to further our understanding of complex surface-atmospheric interactions. The LSMs currently available in ARPS are compared in the next two sections.

Kustas et al. (1996) and Kustas et al. (1999) recommend several statistics for quantifying model error. Three statistics are listed as follows:

$$RMSD = \left[\frac{1}{n} \sum_{i=1}^{n} (P_i - O_i)^2 \right]^{0.5} \tag{27}$$

$$MAPD = \frac{100}{\langle O \rangle} \left(\frac{1}{n} \sum_{i=1}^{n} |P_i - O_i| \right) \tag{28}$$

$$MB = \frac{1}{n} \left(\sum_{i=1}^{n} P_i - \sum^{n} O_i \right) \tag{29}$$

The root-mean-square difference (RMSD) is simply the RMS of the differences between predicted estimates, P_i, and observations, O_i. The mean absolute percent difference (MAPD) is a measure of the fraction of error as a ratio of the mean observed value. The mean bias (MB) is simply the difference between the mean predicted and observed values. These measures were applied to the one-dimensional tests.

4.1 Validation data

The Oklahoma Mesonet (Brock et al. 1995) is an observational network of 115 meteorological stations

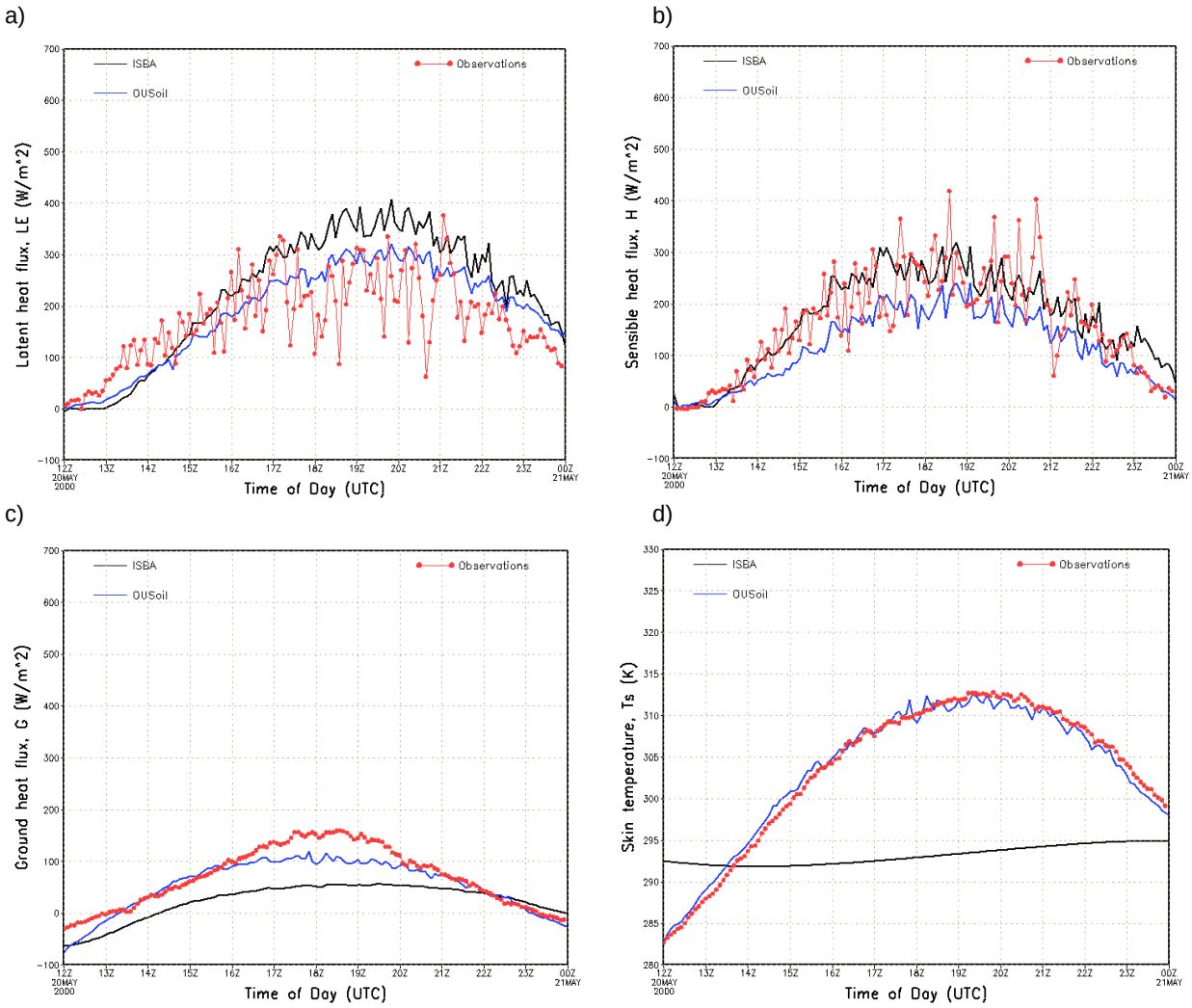

Fig. 1: Model output for the ISBA and OUSoil LSMs plotted against observations collected at NORM during 20 May, 2000. Data include a) latent heat, b) sensible heat, and c) ground heat fluxes (W m^{-2}), and d) skin temperature (°K).

across Oklahoma that collect, archive, and quality control atmospheric, surface, and soil data. Atmospheric pressure, air temperature, relative humidity, precipitation, and wind speed and direction are recorded every 5-minutes; soil moisture and temperature are recorded at four depths (5 cm, 25 cm, 60 cm, and 75 cm) every 30 minutes. During late 1999, the Oklahoma Atmospheric Surface-layer Instrumentation System (Brotzge et al. 1999) outfitted 90 Mesonet sites with additional sensors to record net radiation, surface, and ground heat fluxes, and skin temperature. Ten of these 90 sites, also referred to as "super sites", were equipped with additional ground flux sensors. The flux sensors provided 5-minute observations of incoming and outgoing shortwave and longwave radiation, sensible heat, latent heat, and ground heat fluxes. Data collected from two of these ten sites, sites located near Norman (NORM) and Burneyville (BURN), were used in this study. NORM (Lat. 35° 15' 20"; Lon. 97° 29' 0") is characterized by flat terrain (~0.0° slope) and short grasses and weeds such as goldenrod, bluestem, and ragweed. BURN (Lat 33° 53' 38"; Lon 97° 16' 9") consists of flat pasture land (0.806 slope) with Bermuda grass and Japanese brome. Data archived from 1 January to 31 December, 2000, were available for this verification work. For more site information and photographs, see http://www.mesonet.ou.edu/siteinfo/.

All data were calibrated and quality controlled as described by Brotzge and Weber (2002). Standard Mesonet data were further quality assured by a series of automated and manual checks (Shafer et al. 2000). Redundant instrumentation at the super sites allowed most missing flux data to be replaced; for example, during precipitation events, data are unavailable from the sonic anemometer. Thus, sensible heat flux estimates were replaced using a gradient profile technique (Brotzge and Crawford

Table 1: Statistics of the differences between the ISBA and OUSoil scheme results and Mesonet observations. The root-mean-square difference (RMSD), the mean absolute percent difference (MAPD), and the mean bias (MB) were estimated for each site for each day examined.

		RMSD (W m^{-2})/(K)		MAPD (W m^{-2})/(K)		MB (W m^{-2})/(K)	
		ISBA	OUSoil	ISBA	OUSoil	ISBA	OUSoil
May 20, 2002							
NORM	LE	11.6	4.7	44.5	30.2	50.9	15.4
	H	27.2	12.3	25.2	31.7	9.1	-43.6
	G	32.6	44.8	69.8	27.0	-46.0	-15.6
	Ts	9.76	0.11	3.9	0.3	-10.4	-0.0
	Rn-H-LE-G	85.9	65.33			-15.6	42.4
BURN	LE	326.7	148.9	245.4	113.4	272.9	119.9
	H	168.4	162.6	56.6	59.7	-124.6	-141.3
	G	49.5	27.6	59.7	58.7	29.4	21.1
	Ts	14.3	11.0	4.1	3.0	-12.9	-9.5
	Rn-H-LE-G	168.2	46.2			-139.0	39.1
Aug 1, 2002							
NORM	LE	76.9	56.7	27.9	20.0	15.7	-40.1
	H	52.9	36.5	33.1	21.9	21.9	9.6
	G	30.4	35.2	56.8	54.6	-18.2	-22.8
	Ts	2.02	3.32	0.6	0.8	-1.27	1.73
	Rn-H-LE-G	107.3	69.2			-15.1	57.5
Aug 2, 2002							
BURN	LE	3.3	5.1	39.7	22.3	-109.5	-31.1
	H	166.9	33.5	166.5	29.3	137.9	-17.3
	G	81.1	47.8	155.0	73.2	25.0	11.4
	Ts	1.12	1.36	0.4	0.9	-1.26	-2.62
	Rn-H-LE-G	125.3	53.8			-54.1	36.3

2000). If no redundant instrumentation was available, (e.g., ground heat flux or soil moisture), missing hourly data were linearly interpolated. For this study, latent heat flux was estimated as the residual of the surface energy budget in order to satisfy closure.

The Norman Mesonet site is located approximately 3.03 km to the northwest of a National Weather Service ASOS site and rawinsonde location. Twice daily soundings at 00 and 12 UTC were used for model initialization of the base state. Rawinsonde information collected at NORM (note NORM is different than the NWS site) also was used to initialize model runs for BURN. Vegetation data were obtained from bi-weekly NDVI values from which the appropriate 1 km x 1 km pixel was extracted to coincide with the site locations. These estimates were interpolated to daily values.

4.2 One-dimensional test results

Four one-dimensional simulations were conducted to test the ISBA and OUSoil LSM schemes. Each model run was initialized at 12 UTC and the forecast extended to 12 hours. One spring case and one autumn case were tested at both the NORM and at BURN sites. For the NORM spring case, 75 soil levels were chosen for OUSoil, each soil layer 1 cm in thickness. For the NORM fall case, 10 soil levels were chosen, each 10 cm in thickness. Both BURN cases used 90 soil levels, each 1 cm in thickness. The number of soil levels was varied to test the sensitivity of the soil parameters to the forecast soil temperature and moisture. The ISBA scheme was limited to only 2 soil levels. Each model run was tested once with the ISBA scheme and repeated with the OUSoil scheme. A summary of all statistics from the four one-dimensional tests is provided in Table 1.

The spring NORM case was run using data from 20 May, 2000 (Fig. 1). Results indicate that OUSoil improved modeled surface fluxes and skin temperature significantly over those from the ISBA. For example, LE was estimated as large as 400 W m^{-2} by the ISBA scheme whereas OUSoil estimated a maximum LE near 300 W m^{-2}. Daytime observations of LE oscillated between 200 and 300 W m^{-2}. Model estimates of H are mixed, with the ISBA peaking near 300 W m^{-2} and the OUSoil reaching 225 W m^{-2}. Observations of H varied widely during the day, averaging between 200 and 300 W m^{-2}.

Due to the enhanced resolution of the vertical soil column, significant improvement in G was expected from the OUSoil scheme. Results of OUSoil (Fig. 1.c) indeed showed much closer

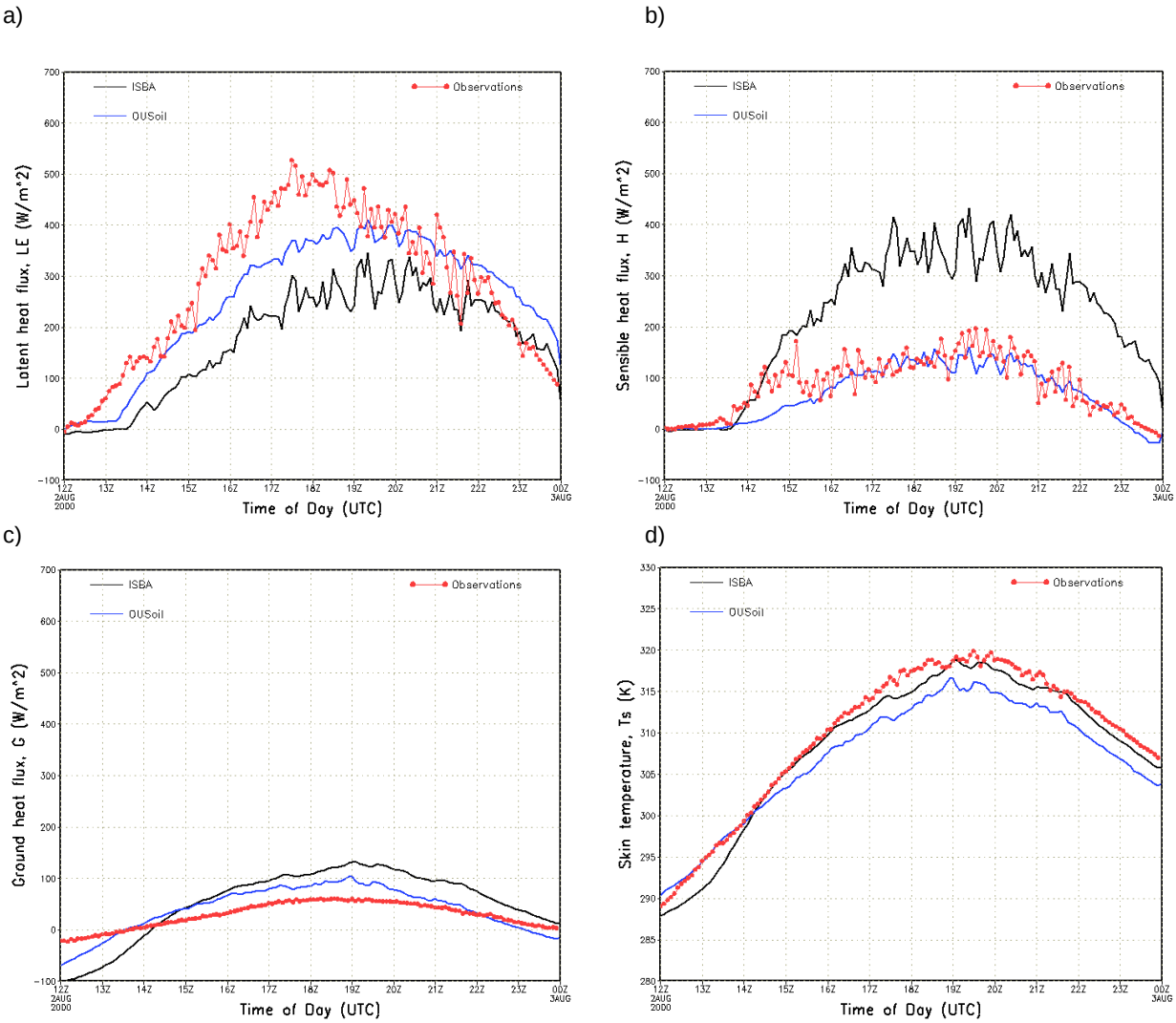

Fig. 2: Model output for the ISBA and OUSoil LSMs plotted against observations collected at BURN during 2 August, 2000. Data include a) latent heat, b) sensible heat, and c) ground heat fluxes (W m^{-2}), and d) skin temperature (°K).

agreement with the observations than did the ISBA. OUSoil showed an approximate 30 W m^{-2} improvement in the daily mean of G.

An examination of the skin temperature also showed very significant improvement by OUSoil over the ISBA scheme. OUSoil predictions of T_s were nearly coincident with observed values (MB ~ 0° C), whereas ISBA estimates remained nearly flat during the day with little diurnal variation (MB > 10° C). The ISBA scheme computes G analytically as a function of T_s, and because of the relatively low temperature difference between T_s and T_2, skin temperature estimates change little with time. On the other hand, T_s is estimated as a direct function of radiative forcing by OUSoil, and the results shown in Fig. 1d reflect the diurnal cycle.

Model runs were repeated on 20 May, 2000, for the BURN site (not shown). Results from both schemes were poor compared to observed values. Nevertheless, OUSoil did improve model results of LE and G over those from ISBA. Neither model succeeded in reproducing T_s values, and subsequently both produced poor estimates of H.

A second day was tested during the fall of 2000 during senescence. The ARPS was initialized for 1 August, 2000 at NORM and run for 12 hours (not shown). Results from the two schemes were fair with errors in LE and H ranging from 20 to 30+%. Results from OUSoil show slight improvements in LE, H, and G when compared to ISBA.

The ARPS was initialized for 2 August, 2000, for BURN and again run for 12 hours (Fig. 2). Results from OUSoil again show some improvement in estimates of LE, H, and G over the ISBA scheme.

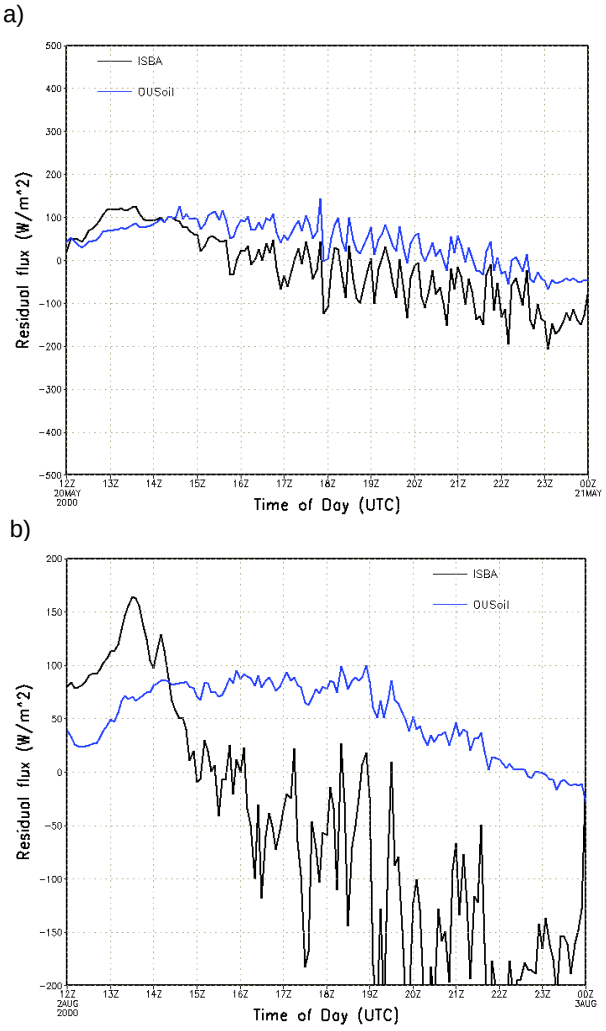

Fig. 3: Residual of the surface energy budget (W m^{-2}; Resid = Rn – LE – H – G), estimated as a function of time of day. Model output of the ISBA and OUSoil LSMs are plotted for a) 20 May, 2000, and b) 2 August, 2000.

While neither scheme captured the 1750 UTC peak in LE at 500 W m^{-2}, the OUSoil scheme peaked at 400 W m^{-2} compared to 300 W m^{-2} by the ISBA scheme. OUSoil estimates of H reflected observations throughout much of the day at about 150 W m^{-2}. ISBA overestimated H by over 200 W m^{-2}. ISBA also overestimated G at midday by about 30 W m^{-2} compared to OUSoil. However, estimates of T_s by ISBA are closer to observations than estimates from OUSoil by several degrees during much of the day.

One major advantage of the OUSoil scheme is that much greater closure is realized than was achieved using the ISBA scheme. (Closure is achieved when Rn – H – LE – G = 0.) Both schemes estimate all components of the energy budget flux independently, so that closure of the energy budget is not guaranteed. Closure estimates from 20 May at NORM and 2 August at BURN are plotted in Fig. 3. In

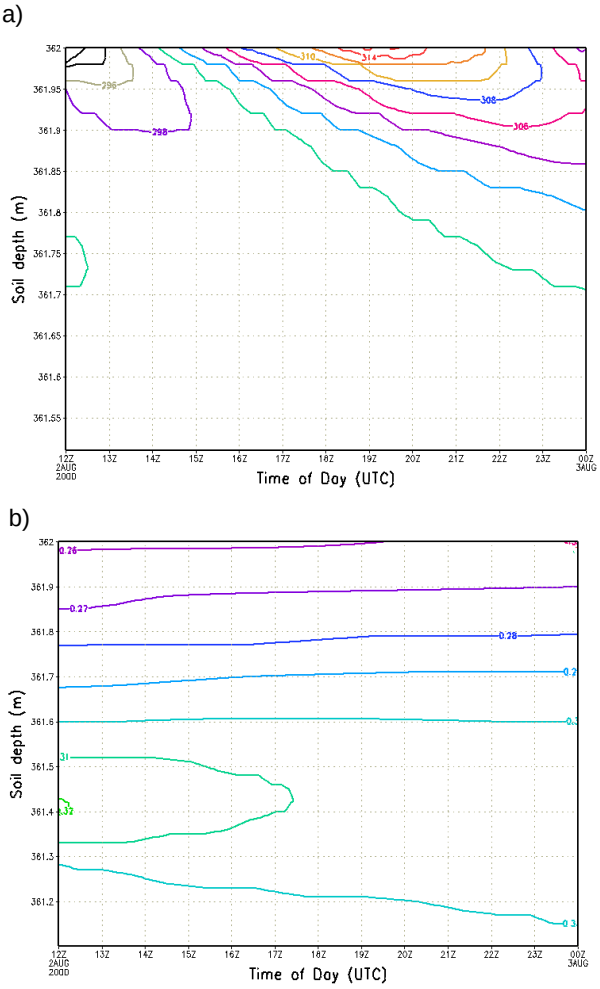

Fig. 4: A time series of the vertical distribution of a) soil temperature (K), and b) soil water content (m^3 m^{-3}) plotted as a function of time of day. Model output from the OUSoil LSM initialized for BURN at 1200 UTC, 2 August, 2000.

both cases, the ISBA scheme significantly overestimated the outgoing energy (residuals << 0). Results from OUSoil show daily means of 35 to 55 W m^{-2} of incoming energy are not used by H, LE, or G. Nevertheless, OUSoil keeps the energy budget much closer to zero during the day than is achieved using ISBA.

A second major advantage of the OUSoil scheme is the high-resolution treatment of the vertical soil column. For the 1-D test runs, and with operational, real-time runs using the ETA EDAS output, the soil column can be initialized at four depths (Fig. 4). The temperature and moisture diffusion equations readily allow for heat and moisture transfer within the column. The time series shown in Fig. 4a shows radiative cooling and heating as a function of the diurnal cycle. Fig. 4b shows drying of the soil column with time.

A major disadvantage of the OUSoil scheme is the added computational needs required by the newer, more sophisticated LSM. The total CPU requirements to run a 12-hour 1-D simulation increased by nearly 17% when replacing the simpler ISBA scheme with a 20-layer OUSoil scheme. Thus, the increase in accuracy must be weighed against the increased computational requirements when choosing among several LSM options..

4.3 Fully coupled, 3-D simulations

A fully coupled, 3-D test case was run using archived data collected from 25 May, 1998. The domain included much of the continental United States, from approximately the Mississippi river westward to just west of the Rocky Mountains with a horizontal grid resolution of 32 km. The model run was initialized at 00 UTC and ran for 24 hours. Model surface temperature and moisture were bi-linearly interpolated to nearby ASOS stations for comparison. Data from approximately 450 stations were examined at 12 UTC, 25 May and 00 UTC, 26 May, 1998.

Model temperature and moisture forecast data were compared to observations as a function of vegetation and soil type. Each model run was repeated twice, first using the ISBA scheme, and then a second time using the OUSoil scheme. Differences between model data and observations were computed, and then averaged across like vegetation and soil types. Calculations of the surface energy budget are implicitly a function of the a priori soil and vegetation type classifications.

An examination of the temperature forecasts by ARPS (not shown) revealed significant degradation in surface temperature forecasts by the OUSoil scheme. Similar results were found for the 12 hour and 24 hour forecasts. Bias estimates between model and observed data reveal that the surface temperature cools too much at night and warms too quickly during the day. Most likely, a problem with the radiation code exists as part of the implementation of the new OUSoil scheme.

Moisture forecasts by ARPS (Fig. 5) showed some improvement by the OUSoil scheme over the ISBA scheme within the first 12 hours. Differences between model estimates and observations averaged as a function of vegetation type indicate a dry bias with the ISBA scheme across most vegetation surfaces (Fig. 5a). The OUSoil scheme improved q predictions across most vegetation types. By 24 hours, however, q estimates increased significantly, regardless of the LSM used (Fig. 5b). A moist bias is evident in predictions of q at 24 hours.

Estimates of q are similarly examined as averaged as a function of soil type. At 12 hours, the OUSoil scheme significantly improved estimates of q across nearly all soil types, and removed much of the dry bias. At 24 hours, however, the OUSoil scheme increased predictions of q across all soil types (except over water), with mixed results when compared against observed values. This large increase in q during the day by the OUSoil scheme is again likely caused by radiation errors and improved performance is expected with a bug fix applied to the radiation code. Updated results will be presented at the AMS conference in February 2003.

5. CONCLUSIONS

Two land surface model schemes, the Interactions Soil Biosphere Atmosphere model and the modified NOAH land surface scheme, OUSoil, were directly compared against observed surface and soil data. Several uncoupled, 1-D model runs were used to examine first-order differences between the two LSMs. Several clear days were chosen at two different observing sites. Results showed some significant improvement in surface temperature and fluxes by the newer OUSoil scheme compared to the original ISBA scheme.

A fully coupled, 3-D model forecast was performed across a limited continental scale region for a 24-hour period. Model predictions of temperature and moisture were compared against observations collected at 450 ASOS sites. Results showed significant temperature error with the new LSM scheme, most likely due to a bug in the radiation code created by the implementation of the OUSoil scheme. An examination of the moisture field revealed some improvement in forecasts of q by the OUSoil scheme by 12 hours, but the temperature errors mask improvement in moisture by the 24 forecast period.

The results of this study highlighted several important issues. First, increased model resolution of the soil column enhances the LSM response to the surface forcing and provides additional understanding on the depth of influence from a single diurnal cycle. It is clear from the results that the ISBA scheme cannot properly represent the transfer of heat and moisture within the top 25cm. Second, LSM behavior is sensitive to vegetation and soil model specification parameters, in particular, the simulations conducted for the Burneyville site were far less effective at representing the soil model response than at the Norman site. Overall, the new scheme performed better than the ISBA scheme, but further study is needed to improve the forecasts over sandy soil regions (Burneyville). Furthermore, the ISBA scheme contains a slow response bias to sunrise that is not apparent, or largely reduced, in the modified NOAH scheme and the results presented in this work is consistent with our experience running the ISBA scheme within a daily ARPS forecast system. The improved response to sunrise by the modified NOAH scheme is due primarily to the existence of a skin temperature equation that contains a small and more appropriate amount of heat capacity. Issues that need to be addressed in future research include: solve the excess radiation forcing problem with the current three-dimensional implementation of the

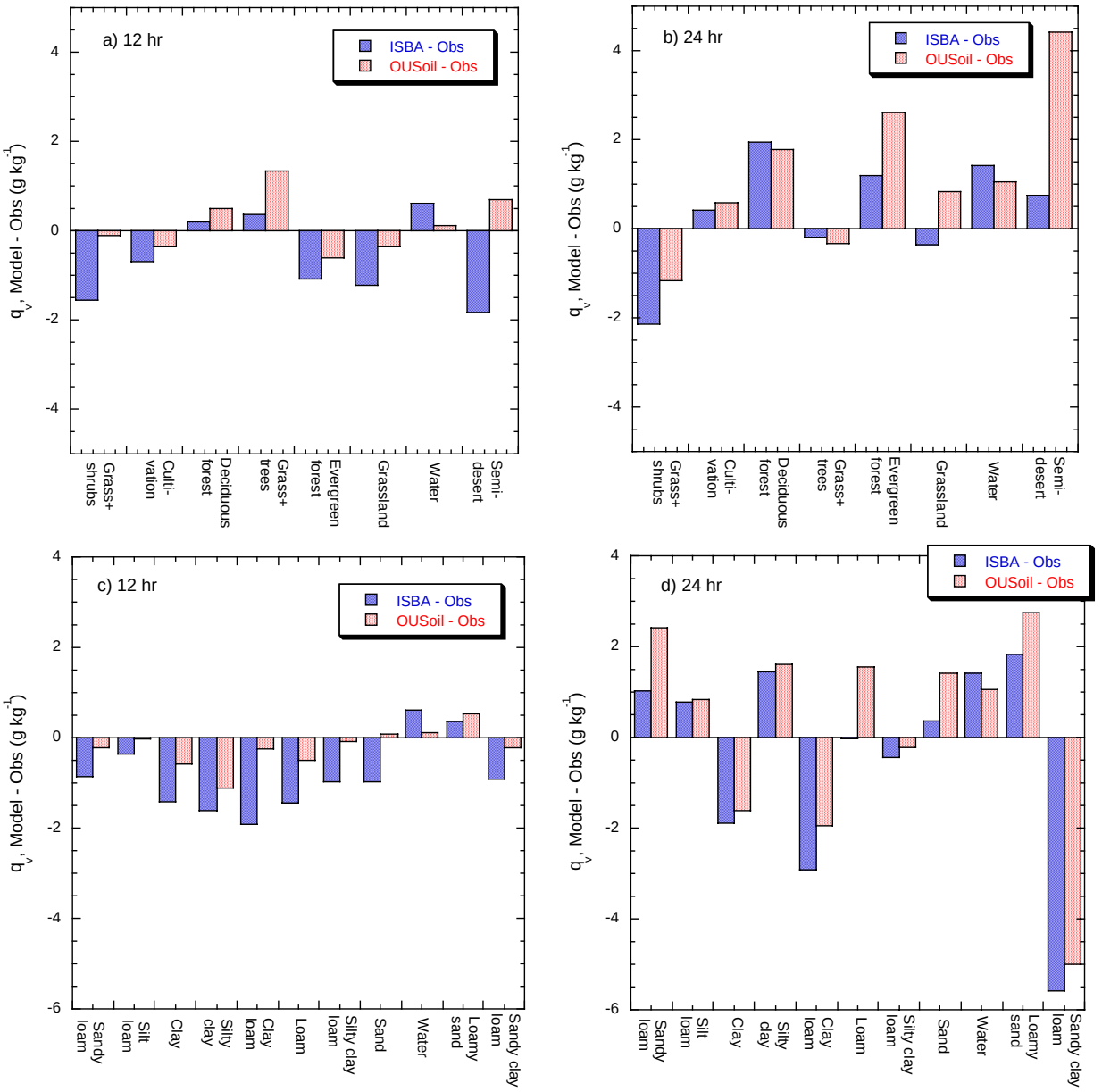

Fig. 5: Mean differences are estimated between model forecasts and ASOS observations collected 25 May, 1998. Forecast estimates for a) 12 hours and b) 24 hours are plotted as a function of vegetation type. Forecast estimates also are plotted for c) 12 hours and d) 24 hours as a function of soil type.

modified NOAH model, further investigate the ability of the LSMs to simulate surface processes over an increasingly diverse set of surface properties, and perform real-time verification to develop a climatology of model results to further identify and improve the LSM performance.

Acknowledgements. The authors would like to thank Bill Martin for providing the ASOS temperature and moisture data for the 3-D verification study. The authors would also like to thank the Oklahoma Climatological Survey for their professional assistance in maintenance, ingest, and quality control of the Mesonet data, and a special thanks goes to the taxpayers of Oklahoma for their continued support and funding of the Oklahoma Mesonet.

REFERENCES

Betts, A. K., J. H. Ball, and A. C. M. Beljaars, 1993: Comparison between the land surface response of the European Centre model and the FIFE-1987 data. *Q. J. R. Meteorol. Soc*., **119**, 975 - 1001.

Betts, A. K., F. Chen, K. E. Mitchell, and Z. I. Janjic, 1997: Assessment of the land surface and boundary layer models in two operational versions of the NCEP Eta model using FIFE data. *Mon. Wea. Rev.,* **125**, 2896 – 2916.

Brock, F. V., K. C. Crawford, R. L. Elliott, G. W. Cuperus, S. J. Stadler, H. L. Johnson, and M. D. Eilts, 1995: The Oklahoma Mesonet: A technical overview. *J. Atmos. Oceanic Technol*., **12**, 5 - 19.

Brotzge, J. A., and K. C. Crawford, 2000: Estimating sensible heat flux from the Oklahoma Mesonet. *J. Appl. Meteor*., **39**, 102-116.

Brotzge, J. A., S. J. Richardson, K. C. Crawford, T. W. Horst, F. V. Brock, K. S. Humes, Z. Sorbjan, and R. L. Elliott, 1999: The Oklahoma Atmospheric Surface-layer Instrumentation System (OASIS) project. Preprint, 13th Conf. On Bound.-Layer Turb. Dallas, TX, Amer. Meteor. Soc., 612 – 616.

Brotzge, J. A., and D. Weber, 2002: Land-surface scheme validation using the Oklahoma Atmospheric Surface-layer Instrumentation System (OASIS) and Oklahoma Mesonet data: Preliminary results. *Meteor. Atmos. Phys*., **80**, 189 - 206.

Chen, F., and J. Dudhia, 2001: Coupling an advanced land surface-hydrology model with the Penn State-NCAR MM5 modeling system. Part I: Model implementation and sensitivity. *Mon. Wea. Rev*., **129**, 569 – 585.

Chen, T. H., A. Henderson-Sellers, P. C. D. Milly, A. J. Pitman, A. C. M. Beljaars, J. Polcher, F. Abramopoulos, A. Boone, S. Chang, F. Chen, Y. Dai, C. E. Desborough, R. E. Dickinson, L. Dumenil, M. Ek, J. R. Garratt, N. Gedney, Y. M. Gusev, J. Kim, R. Koster, E. A. Kowalczyk, K. Laval, J. Lean, D. Lettenmaier, X. Liang, J.-F. Mahfouf, H.-T. Mengelkamp, K. Mitchell, O. N. Nasonova, J. Noilhan, A. Robock, C. Rosenzweig, J. Schaake, C. A. Schlosser, J.-P. Schulz, Y. Shao, A. B. Shmakin, D. L. Verseghy, P. Wetzel, E. F. Wood, Y. Xue, Z.-L. Yang, and Q. Zeng, 1997: Cabauw experimental results from the Project for Intercomparison of Land-Surface Parameterization Schemes. *J. Climate,* **10**, 1194-1215.

Deardorff, J. W., 1978: Efficient prediction of ground surface temperature and moisture, with inclusion of a layer of vegetation. *J. Geophys. Res*., **83**, 1889 - 1903.

Ek, M., and L. Mahrt, 1991: OSU 1-D PBL model user's guide. Version 1.04, 120 pp. [Available from Department of Atmospheric Sciences, Oregon State University, Corvallis, OR 97331-2209.]

Henderson-Sellers, A., Z.-L. Yang, and R. E. Dickinson, 1993: The Project for Intercomparison of Land-Surface Parameterization Schemes. *Bull. Amer. Meteor. Soc*., **74**, 1335 - 1349.

Kustas, W. P., K. S. Humes, J. M. Norman, and M. S. Moran, 1996: Single and dual-source modeling of surface energy fluxes with radiometric surface temperature. *J. Appl. Meteor.,* **35**, 110 – 121.

Kustas, W. P., and J. M. Norman, 1999: Evaluation of soil and vegetation heat flux predictions using a simple two-source model with radiometric temperatures for partial canopy cover. *Ag. For. Meteor*., **94**, 13 – 29.

McCumber, M. C., and R. A. Pielke, 1981: Simulation of the effects of surface fluxes of heat and moisture in a mesoscale numerical model. *J. Geophys. Res*., **86**, 9929 – 9938.

Noilhan, J., and S. Planton, 1989: A simple parameterization of land surface processes for meteorological models. *Mon. Wea. Rev*., **117**, 536 - 549.

Peters-Lidard, C. D., E. Blackburn, X. Liang, and E. F. Wood, 1998: The effect of soil thermal conductivity parameterization on surface energy fluxes and temperatures. *J. Atmos. Sci*., **55**, 1209 – 1224.

Pleim, J. E., and A. Xiu, 1995: Development and testing of a surface flux and planetary boundary layer model for application in mesoscale models. *J. Appl. Meteor.,* **34**, 16-32.

Qu, W., A. Henderson-Sellers, A. J. Pitman, T. H. Chen, F. Abramopoulos, A. Boone, S. Chang, F. Chen, Y. Dai, R. E. Dickinson, L. Dumenil, M. Ek, N. Gedney, Y.M. Gusev, J. Kim, R. Koster, E. A. Kowalczyk, J. Lean, D. Lettenmaier, X. Liang, J.-F. Mahfouf, H.-T. Mengelkamp, K. Mitchell, O. N. Nasonova, J. Noilhan, A. Robock, C. Rosenzweig, J. Schaake, C. A. Schlosser, J.-P. Schulz, A. B. Shmakin, D. L. Verseghy, P. Wetzel, E. F. Wood, Z.-L. Yang, and Q. Zeng, 1998: Sensitivity of latent heat flux from PILPS land-surface schemes to perturbations of surface air temperature. *J. Atmos. Sci*., **55**, 1909 – 1927.

Shafer, M. A., C. A. Fiebrich, D. S. Arndt, S. E. Fredrickson, and T. W. Hughes, 2000: Quality assurance procedures in the Oklahoma Mesonetwork. *J. Atmos. Oceanic Technol.,* **17**, 474 - 494.

Smirnova, T. G., J. M. Brown, and S. G. Benjamin, 1997: Performance of different soil model configurations in simulating ground surface temperature and surface fluxes. *Mon. Wea. Rev.,* **125**, 1870 – 1884.

Xiu, A., and J. E. Pleim, 2001: Development of a land surface model. Part I: Application in a mesoscale meteorological model. *J. Appl. Meteor*., **40**, 192 – 209.

Xue, M., K. K. Droegemeier, and V. Wong, 2000: The Advanced Regional Prediction System (ARPS) – A multi-scale nonhydrostatic atmospheric simulation and prediction model. Part I: Model dynamics and verification. *Meteor. Atmos. Phys*., **75**, 161 – 193.

Xue, M., K. K. Droegemeier, V. Wong, A. Shapiro, K. Brewster, F. Carr, D. Weber, Y. Liu, and D. Wang, 2001: The Advanced Regional Prediction System (ARPS) – A multi-scale nonhydrostatic atmospheric simulation and prediction model. Part II: Model physics and applications. *Meteor. Atmos. Phys*., **76**, 143 – 165.